Comparison of lever arm determination methods in terms of their effect of the accuracy of aerial triangulation

Ágnes KRAUSZ
Institute of Geoinformatics
Óbuda University, Alba Regia Technical Faculty
Székesfehérvár, HUNGARY
krauszagi@gmail.com

Gergely LÁSZLÓ
Institute of Geoinformatics
Óbuda University, Alba Regia Technical Faculty
Székesfehérvár, HUNGARY

Department of Orthophotogrammetry,
Envirosense Hungary Ltd.
Debrecen, HUNGARY
laszlo.gergely@amk.uni-obuda.hu

***Abstract*— With the help of aerial remote sensing, especially when we are talking about large aircraft surveys, we can collect a large amount of information from a large area in a short time. In order for the resulting, in our case, photo-based (photogrammetric) data to be used for engineering purposes, it is important to ensure their accuracy. One of the components of this, in addition to an appropriately accurate camera model, is knowing the 3D position of the photographs and their spatial position with great accuracy. Knowing these, we can perform aerial triangulation. Since these data cannot be measured directly, we need to know the eccentricity vectors of the measuring devices (GNSS/IMU) with respect to the main points of the cameras.**

In this study, we will examine the effect of the accuracy of different measurement methods (engineering geodesy, laser scanning, software estimation) on the results of aerial triangulation.

Keywords— lever arm, aerial triangulation, photogrammetry, laser scanning, engineering geodesy

I. INTRODUCTION

Remote sensing is used for data collection when we cannot or do not want to work directly in the area to be surveyed. In order for a large part of the field measurements to be substituted, it is important that the accuracy of the remotely sensed data does not fall short of that available with field data collection procedures. To fulfill this aspect, our remotely sensed data must meet several criteria. For example, they are suitable if the followings are known:

- ground sample distance (GSD)
- depending on the final product, image overlap relative to each other
- sensor parameters known with sufficient accuracy
- coordinates of data collection locations determined with high precision and the spatial angle of the collected data in some known projection system, and designated direction
- and, of course, the appropriate data collecting conditions

If we are talking about photo-based aerial remote sensing, then we can ensure the desired field resolution by knowing the parameters of the measuring camera (internal orientation elements: pixel size, sensor size, focal length, principal point coordinates, distortions parameters), based on a topography model, and calculating the appropriate flight height.

Some of the required camera parameters (pixel size in millimeters, sensor size, nominal focal length) are determined by the camera and lens type, while the rest (principal point coordinates, actual focal length, distortions parameters) require camera calibration.

To plan data collection with the required overlap, in addition to the method of use of the final product (e.g.: orthophoto, true ortho), which determines the amount of overlap to be used, we also need the calibrated parameters of the camera sensor and the previously calculated flight height.

Adequate data acquisition conditions can be achieved if a sensor suitable for the purpose is used under ideal environmental conditions (weather, time of day).

Knowing the data collection locations is important because in photogrammetry - or in any remote sensing procedure - the basic task is to be able to produce field coordinates from the image coordinates of recordings, thus making it possible to carry out measurements on them. To do this, we need to determine exactly where the projection center of the camera was located in space (interpreted in a given projection) at the time of recording. If we also know the orientation of the image plane, then we know all the external orientation elements ($x,y,z;\omega,\varphi,\kappa$) in order to perform field coordinate calculations from pixel coordinates.

The problem with the above point is that the external orientation elements can only be determined indirectly, with separate sensors (GPS, IMU), not directly in the projection center or in the image plane, so the measured values are always burdened by eccentricity. For smaller, more compact systems, such as UAV survey systems, these eccentricity vectors are defined and published by the manufacturer, but for large-scale aerial photography, especially if the sensor configuration changes frequently, they need to be determined and checked regularly.

In this study, the authors present the traditional, geometric way of determining the eccentricity vectors, as well as the developed algorithm, which automatically enables the calculation of these vectors using an analytical method.

II. Lever Arm measurement with Total Station

We can perform the measurement when the sensors are installed in the aircraft. The measurement is carried out using an engineering geodesic method, typically with a total station. In order for the eccentricity vectors and the rotation angles to be properly interpreted, in addition to the sensors, a reference plane and a reference direction must also be measured. In our case, the reference plane was the base plate holding the sensors, while the direction was the longitudinal axis of the fuselage. Overall, the following points are measured:

- base plate flat, with three points (bore holes A, B, C) (Fig. 1)

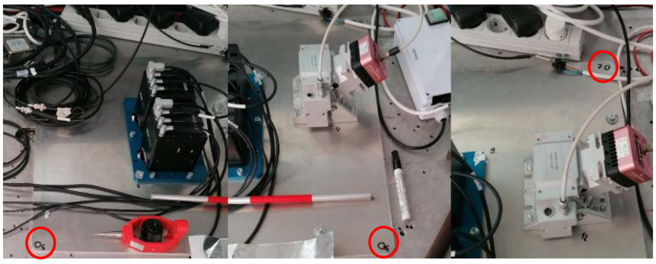

2. Figure Points on plate, boreholes: point A, B and C

- plane longitudinal axis, with two points (t1, t2) (Fig. 2)

3. Figure Points on plane, endpoints of axis line

- inertial measurement unit, depending on the type, with one or two points (IMU) (Fig. 3)

1. Figure Point on IMU

- camera (fixing frame), with two points (cph1, cph2) (Fig. 4)

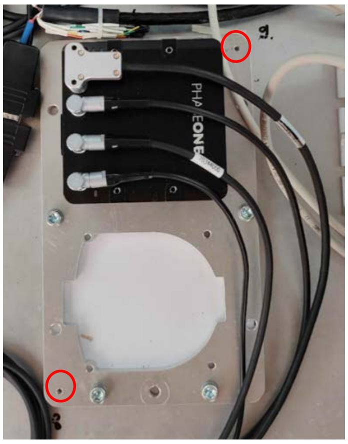

4. Figure Points of camera

- hyperspectral camera, with two points (hs1, hs2) (Fig. 5)

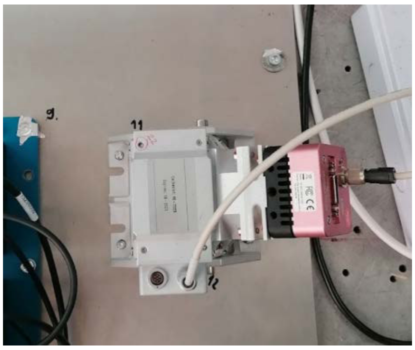

5. Figure Points on Hyper

-In Figure 6. two GPS antennas, with one point each (ant1, ant2)

6. Figure Points of the antennas

During the measurement, we stand next to the plane with the instrument in such a way that both the outer and inner points are visible at the same time, in five rounds it takes place in one face, using a propped-up miniprism, with a 300 mm extension rod at some points if necessary.

III. PROCESSING WITH TRADITIONAL, GEOMETRIC METHOD

We start the processing by averaging the five-round measurement. Thus, if at any point we experience an error in the measurement results, we have the option to remove such values.

The coordinate list obtained in this way is imported point by point into AutoCAD, then for easier work we also place labels next to the points with point numbers and then group them by using layer allocation.

By connecting the points of the plane, we create a plate, then we also connect the axis points so that we can use them as a reference line.

We create a user coordinate system by shifting so that the XY plane contains the plane of the base plate, and the origin coincides with one of the measured bore holes (e.g., point A).

After that, the axis-line is moved with its midpoint to the origin, then its start and end points are rotated to the XY plane by zeroing the Z coordinates.

In the next step, we rotate the +X axis in the direction of the aircraft axis so that it faces the propeller.

Using the measured IMU points and the available technical drawings, we draw the reference point of the IMU, to which we move the origin using a repeated coordinate system shift.

In this final, directional reference system, based on the sensor points, using the dimensions of blueprints and 3D models, we determine the position of the camera focal points and the center of mass of the hyperspectral camera with various editing steps.

As a final step, the X, Y, Z coordinates of the transformed points are manually read point by point and recorded in a coordinate list, which can be used to perform the trajectory processing.

IV. LEVER ARM MEASUREMENT WITH LASER SCANNER

Laser scanner measurement differs fundamentally from traditional geodetic surveys in that, while the latter measures selected points, with scanning we only have the option of choosing from which point and which part of the space we want to measure, and the selection of the points we need can only be done during processing.

The planning of the measurement is also different, because due to its structure, it is almost impossible to measure an aircraft from one position in such a way that the GNSS antennas placed on top and the sensors that are of utmost importance for the task are visible, so the measurement must be performed from at least two positions, one of which is also it should be of a high height, relatively close to the plane, as shown in Figure 7.

7. Figure Measurement from elevated station

When measuring the interior of the aircraft, the scanner must be set up with a different approach than a total station, because here, in contrast, it is also important that the sensors are visible as much as possible on the point cloud, so that their geometry can be determined as precisely as possible, for the calculation of the characteristic points. This last clause is particularly important because, while a total station can measure a point in a cover (e.g., drill hole) by raising a prism pole, these points can only be determined indirectly during scanning, based on the surrounding point cloud points. The resolution of the scanning was set to 1x1 mm interpreted at the farthest point of the plane. After the measurement, photographs were also taken for subsequent coloring of the point cloud.

The first step after the measurement was to import the data into the program used for processing (Leica Cyclone). Since the plane was not surveyed from one point of view, it was necessary to transform the stations into each other. Since we used targets during the measurement, which the program recognizes and can automatically use as reference points for the operation, we also have control option over the step. The point cloud (as in Fig. 8) was matched to targets with a mean error of between 1-3 mm, while the automatic point matching procedure between the point clouds gave the following results:

- `Overlap Point Count: 244133`
- `Overlap Error Statistics`
- `RMS: 0.00849298 m`
- `AVG: 0.00400456 m`
- `MIN: 5.20021e-07 m`
- `MAX: 0.0938572 m`

The results tally with the expected values given by the specifications of the instrument and indicate the reliability of the measurement technology to around 4 mm for these set up.

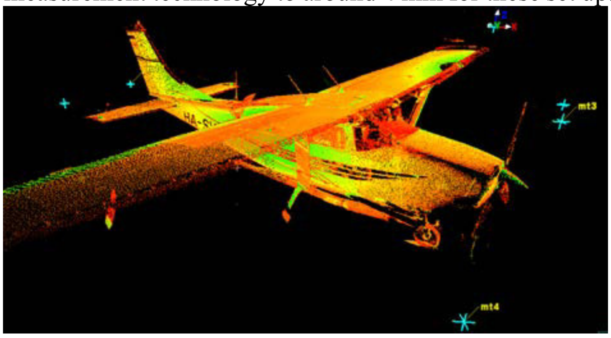

8. Figure Transformed point cloud image of the plane

The transformation of the point cloud was followed by coordinate measurement. This was done in such a way that after identifying the location of the points to be measured, we sorted them together with their immediate surroundings, and then selected with the greatest possible accuracy the point that was most likely the closest to the reference point. After that, we queried the coordinates with object info.

The following figures 9-15. show the measured point on the point cloud:

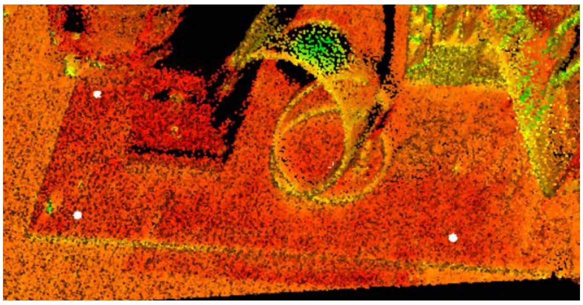

9. Figure Point cloud points on plate

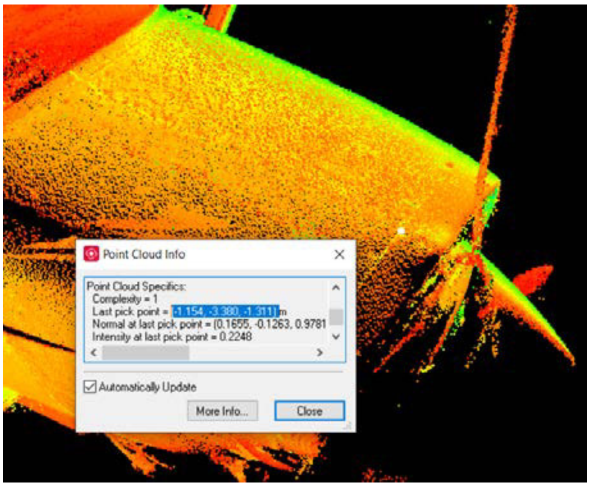

10. Figure Front axis point on the point cloud

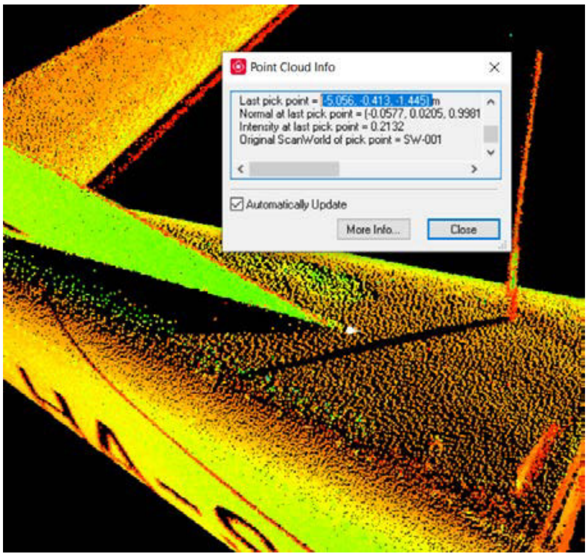

11. Figure Rear axis point on the point cloud

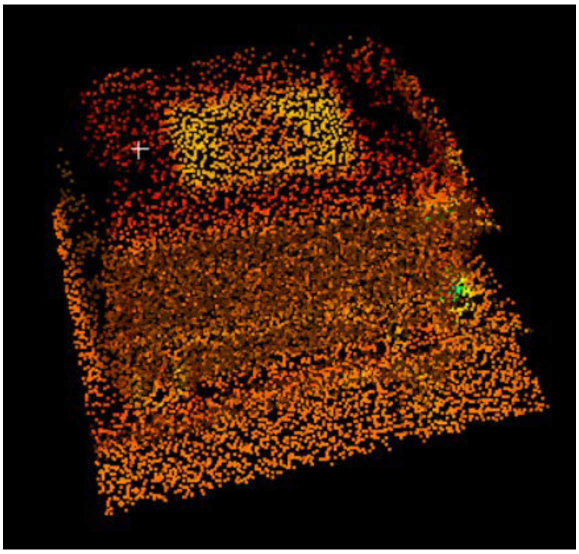

12. Figure IMU and its reference point

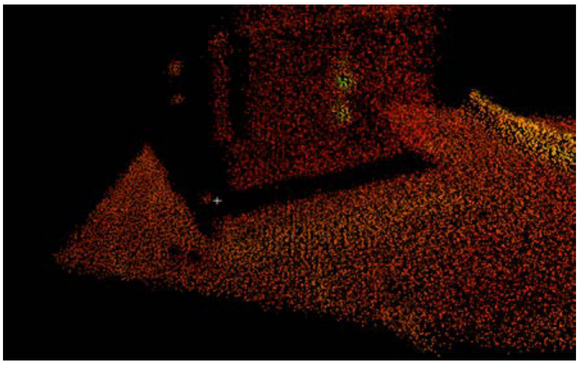

13. Figure Camera with measurement point

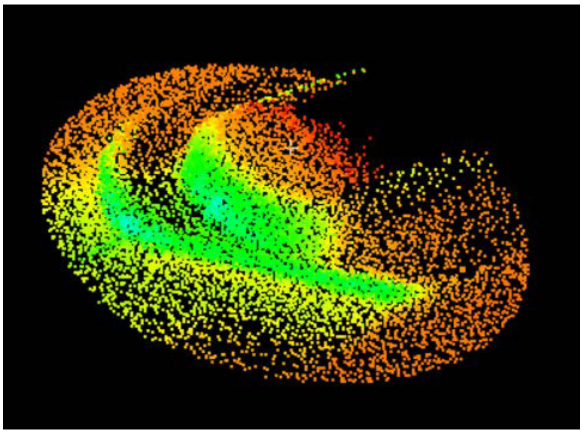

14. Figure Points of the rear GNSS antenna

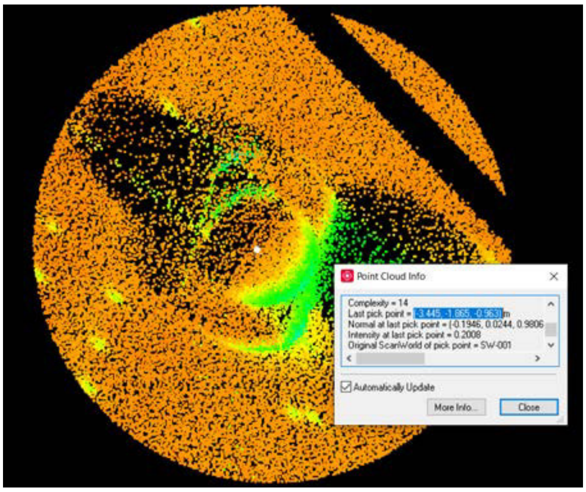

15. Figure Point cloud image of the front GNSS antenna

The coordinates were processed and transformed into the IMU origin coordinate system as described in the total station method.

Point	x	y	z
IMU	0	0	0
Ant b	-0.2773	-0.2831	0.9723
Ant f	-0.3091	0.6114	1.1143
Cam l	-0.1063	0.4680	-0.0152
Cam r	-0.2132	0.4681	-0.0152

1. Table 3D vectors of the Total Station measured sensors (Ant- GNSS Antenna, Cam - Camera, b - Rear, f - Front, l - Left, r - Right)

Pont	x	y	z
IMU	0	0	0
Ant b	-0.2794	-0.2839	0.9740
Ant f	-0.3106	0.6103	1.1161
Cam l	-0.1090	0.4712	-0.0118
Cam r	-0.2108	0.4669	-0.0143

2. Table 3D vectors of the Laser Scanned sensors

Point	Δx	Δy	Δz	Δ3D
IMU	0.0000	0.0000	0.0000	0.000
Ant b	0.0021	0.0008	-0.0017	0.003
Ant f	0.0015	0.0011	-0.0018	0.003
Cam l	0.0027	-0.0032	-0.0034	0.005
Cam r	-0.0024	0.0012	-0.0009	0.003

3. Table Differences of the two measurements

The differences in Tables 1-3. show that the results of the two determinations are very close to each other, the difference is 3 mm on average.

V. Effects of measured lever arm vectors on aerial triangulation results

To carry out the test, we had to choose a flight project that was suitable for testing in terms of its scope and other parameters with the given configuration. Our choice fell on the Nagykáta settlement project, as it had the right configuration and was flown in the afternoon on 04/14/2022, a week earlier than the measurement 04/20/2022, under ideal weather conditions. Since it is a small settlement, the aerial triangulation of the 187-frame project can be done in about 10 minutes, which is useful for such research if it needs to be repeated several times. After selecting the project, we calculated the external orientation elements of the photographs based on the flight trajectory with the sensor coordinates created in IMU system for both cases.

Afterwards, to make the results as comparable as possible, we carried out the identification of Ground Control Points (GCP) on a preliminary aerial triangulation and determined the AT parameters during the test. To not distort the results in any way, the camera calibration was not allowed to be refined during the process.

The test parameters were set as follows:

```
Number of photos              : 187
  Number of strips            : 7

  Photo scale                 : 1:13643
  Mean terrain height [m]     : 156

  Strategy parameter:
  --------------------


  Overview # to start                 : 5
  Overview # to stop                  : 0
  # of pyramid levels to be processed : 6
  # of tie points to be measured
     in last level                    : 3
  Use manual measurements as TPC
     : ON
  Create numeric point id             : ON
  TiePointCenterPattern               : 4 x 4
```

```
TiePoint density                    : default
Thinout size in pixel
   : 50
Try to track points
   from upper levels:               : ON
Matching sequence                   :  FBM  FBM  LSM
                                    SKIP FBM LSM
Number additional threads           : 1
Cache size per thread               : 10 MByte

Working directory                   : .\
DEM for Initialization      :Nagykata_DTM_UTM34.dtm

Matching parameter :
--------------------

FBM-Method:

Matching window                     : 100 x 100
Operator window size                : 5 x 5
Non-max. suppr. window size         : 5
Threshold for correlation coefficient : 0.92
Window for correlation coefficient  : 5 x 5
Wmin                                : 0.10
Qmin (roundness)                    : 0.50
Parallax bound                      : 30
Epipolar line to be used            : ON
Distance to epipolar lines          : 0.50
LSM-Method:

Correlation coefficient             : 0.93
Template size [pixel]               : 21
Edge size [pixel]                   : 6
# of iterations                     : 20


Control parameter for block adjustment:
----------------------------------------

Self-calibration                    : OFF
GNSS-Mode                           : ON
Drift-Mode                          : ON
drift per strip                     : ON
drift for X, Y, Z                   : ON,ON,ON
enable shifts only                  : OFF
IMU-Mode                            : ON
IMU-Boresight                       : ON
Earth's curvature correction        : ON
Atmospheric correction              : ON
Do not eliminate manual points      : ON
Do not eliminate GNSS               : ON
```

Looking at the results in Figures 16-18, in both cases the Sigma 0 value of aerial triangulation was 0.8 microns, which corresponds to 0.2 pixels. This means an average accuracy of 1 cm for a GSD of 5 cm, which is very good.

The residuals of the automatic point matching are also very close to each other in the two cases, based on the histogram no visual difference can be established.

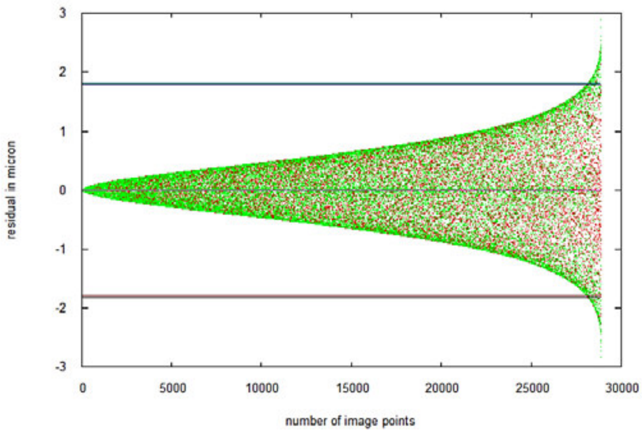

16. Figure Photo residual histogram plot for automatic measured points for Total Station

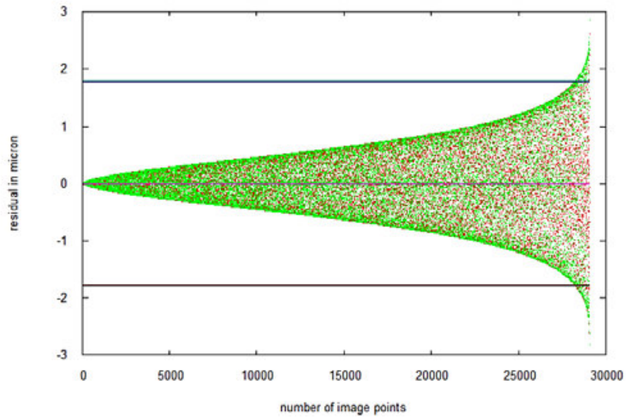

17. Figure Photo residual histogram plot for automatic measured points for Laser Scanner

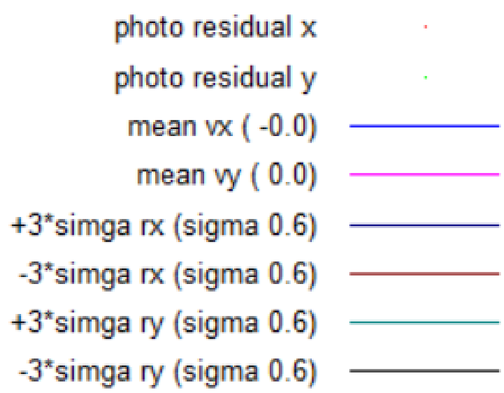

18. Figure Legend for the two histogram plots above

There is a difference of 0.1 micron in the residuals of the camera model in favor of the total station determination method (Fig. 19-20), which is also negligible.

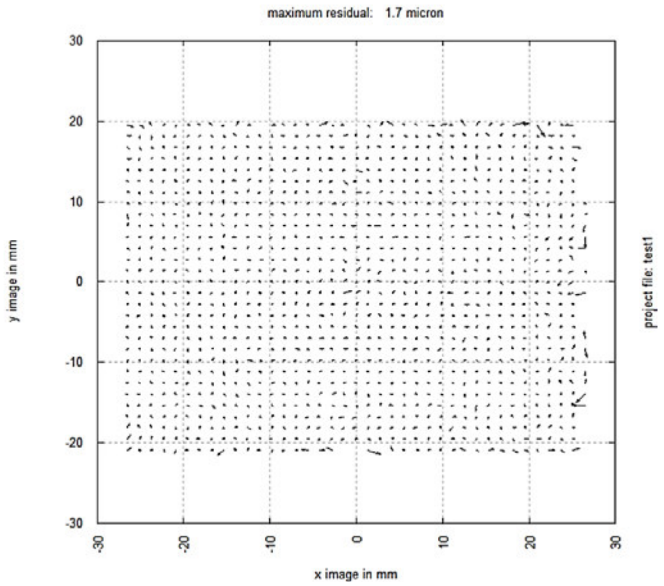

19. Figure Image residual plot for automatic measured points for Total Station

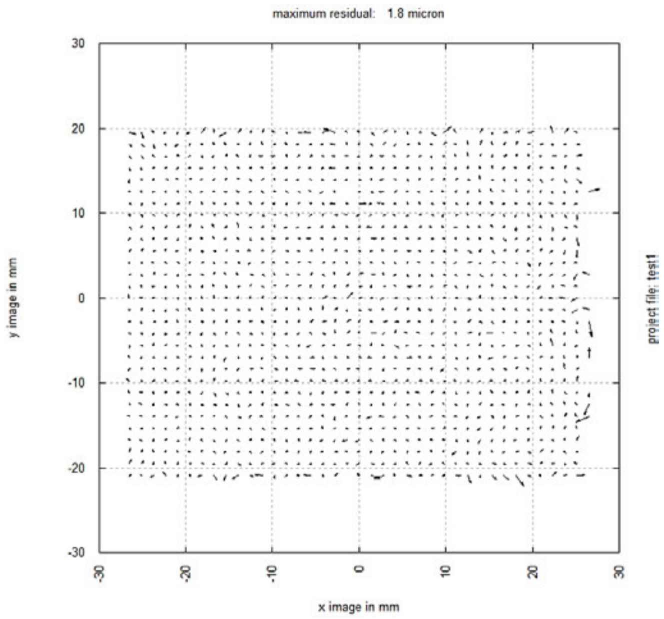

20. Figure Image residual plot for automatic measured points for Laser Scanner

By analyzing the numerical results on Table 4, there are thousandths of micron differences in favor of the laser-scanned method, which can be explained by the fact that the GCP designation was refined on that data set.

		Total Station	Laser Scanner
sigma 0 in micron		0.8	0.8
number block points		8112	8161
number of images		187	187
number of iterations		12	12
redundancy		33859	34036
mean std dev ground	x	0.009 [m]	0.009 [m]
	y	0.009 [m]	0.009 [m]
	z	0.026 [m]	0.026 [m]
mean std dev ori	omega	1.6 [mdeg]	1.6 [mdeg]
	phi	1.6 [mdeg]	1.6 [mdeg]
	kapp	0.7 [mdeg]	0.7 [mdeg]
mean std dev ori	x	0.019 [m]	0.019 [m]
	y	0.019 [m]	0.019 [m]
	z	0.014 [m]	0.014 [m]
rms image points	x	0.594 [micron]	0.590 [micron]
	y	0.603 [micron]	0.597 [micron]
rms control in image	x	1.683 [micron]	1.675 [micron]
	y	2.176 [micron]	2.137 [micron]
rms control in terr	x	0.008 [m]	0.008 [m]
	y	0.007 [m]	0.008 [m]
	z	0.013 [m]	0.013 [m]
max res. control	x	0.015 [m]	0.015 [m]
	y	-0.015 [m]	-0.015 [m]
	z	-0.036 [m]	-0.036 [m]

4. Table Comparison of the AT results of the two measuring methods

VI. SUMMARY, POSSIBLE DEVELOPMENTS

The lever arm measurement is traditionally done with a total station, but the question arose as to whether it could be an advantage if it were done with a laser scanner procedure. The advantage of the latter is that we don't have to bother with identifying the points in the field, this step can be solved in office conditions on the ready-made point cloud. The list of advantages ends here, but there are several important aspects among its disadvantages:

1. the planning of the measurement requires even more attention and therefore time,
2. the measurement with maximum accuracy settings takes longer than with a measuring station, even with 5 rounds
3. it is not enough to perform the measurement from one station, at least one more position with a view of the top of the plane from a high elevation is necessary
4. if there are several stations, in order to connect them, then the placement of the targets, requires special planning and time
5. target measurement is required at each station, which consumes additional time
6. since even with careful planning, there can be important points that cannot be seen, so additional manual measurements with a ruler or a measuring station may be necessary (which calls into question the viability of the whole method in terms of simplicity)
7. for using several stations, alignment inaccuracy affects the final accuracy
8. during processing, the identification of points (especially those of devices with low reflectance) and

the construction of separately measured parts are time-consuming

9. if there is no reference measurement, it is easy to make (blunder) mistakes

Based on one pair of measurements, it cannot be stated that laser scanning has the right to exist in the topic of lever arm measurement, but neither can the opposite. A new pair of measurements is definitely necessary, preferably with a new reference area for aerial triangulation. With the new measurement, it would be worthwhile to try to perform scanning from only one position, and by placing reflectors on the antennas and internal hidden points, we would "see" it, thus eliminating a significant part of the listed disadvantages (3-8). With this method, we can perhaps get a more complete picture of the applicability of laser scanner measurement for this purpose.

VII. References

[1] János Katona: Parcel analysis for the general application of remote sensing monitoring, In: AIS 2019 : 14th International Symposium on Applied Informatics and Related Areas organized in the frame of Hungarian Science Festival 2019 by Óbuda University, Székesfehérvár: Óbudai Egyetem, pp 69-70 (2019)

[2] Lucas Grégory; Halász László; Solymosi József. Exploring the capacities of airborne technology for the disaster assessment, HADMÉRNÖK 8 : 3 pp. 74-91. , 18 p. (2013)

[3] Lucas Grégory, Considering time in orthophotography production: from a general workflow to a shortened workflow for a faster disaster response, Intenrational Archives of Photogrammetry and Remote Sensing (2002-) XL3 : W3 pp. 249-255. , 7 p. (2015)

[4] Schickler, W., and A. Thorpe, 1998. Operational procedure for automatic true orthophoto generation, International Archives of Photogrammetry and Remote Sensing, 32(Part 4):527-532.

[5] Balázsik V., Tóth Z., Abdurahmanov I. Analysis of Data Acquisition Accuracy with UAV INTERNATIONAL JOURNAL OF GEOINFORMATICS (1686-6576): 17 1 pp 1-10 (2021)

[6] Kugler, Zsófia ; Tóth, Zoltán ; Szalay, Zsuzsa ; Szagri, Dóra ; Barsi, Árpád Supporting microclimate modelling with 3D UAS data acquisition IDŐJÁRÁS / QUARTERLY JOURNAL OF THE HUNGARIAN METEOROLOGICAL SERVICE 123 : 3 pp. 279-294. , 16 p. (2019)

[7] A. Ládai, C. Toth, Z. Tóth INDOOR MAPPING WITH AN OMNIDIRECTIONAL CAMERA SYSTEM: PERFORMANCE ANALYSIS INTERNATIONAL ARCHIVES OF PHOTOGRAMMETRY AND REMOTE SENSING (2002-) XLIII-B1-2022 pp. 347-352. , 6 p. (2022)